Journal of Advanced Ceramics
2014, 3(4): 259–268
DOI: 10.1007/s40145-014-0115-z

ISSN 2226-4108
CN 10-1154/TQ

Research Article

Utilization of iron oxide bearing pellets waste for preparing hard and soft ferromagnetic glass ceramics

Salwa A. M. ABDEL-HAMEED[a,*], Ibrahim M. HAMED[b], Nehal A. ERFAN[b]

[a]*Glass Research Department, National Research Center, Dokki, Cairo, Egypt*
[b]*Chemical Engineering Department, Faculty of Engineering, Minia University, Minia, Egypt*

Received: May 04, 2014; Revised: June 18, 2014; Accepted: June 20, 2014

Abstract: About 8% of the imported iron oxide pellets burdens to Egypt are wasted. In this paper, broken pellets waste (BPW) is used as raw material for the preparation of hard magnetic glass ceramics (HMGC) as well as soft magnetic glass ceramics (SMGC). About 54 wt% and 37 wt% of BPW are used to prepare SMGC and HMGC, respectively. Differential thermal analysis (DTA) reveals two broad exothermic peaks for HMGC at 591 ℃ and 697 ℃, whereas one exothermic peak at 820 ℃ is detected for SMGC. X-ray diffraction (XRD) shows the crystallization of hematite as the sol phase in BPW, and meanwhile, Zn–ferrite and Ba–hexaferrite are identified in SMGC and HMGC, respectively. Transmission electron microscopy (TEM) reveals the crystallization of nanosize particles of ~20 nm for SMGC and ~12 nm for HMGC. Vibrating scanning magnetometer (VSM) reveals an increase in saturation magnetization from ~1 emu/g for BPW to ~77 emu/g for SMGC and 21 emu/g for HMGC.

Keywords: magnetic materials; nanostructure; pellets waste

1 Introduction

Environment and human health effects are intricately linked; therefore, the need for waste recycling is a fact of the healthy life today. Scientists and technologists continue to seek ways to reduce the environmental impact of waste. Despite the economical importance of industry in the development along with its contribution to the improvement of the life quality for millions of people throughout the world, it has been a major source of not only air and water pollution but also industrial pollution resulting from solid waste disposal which consequently leads to environmental inconvenience and wasting money. Owing to the growing amount of solid waste produced by industrial firms and the enforced environmental regulations as well as the need to pollution abatement, an increasing interest has been developed to utilize recycling as a means of diverting solid waste to new useful glass ceramic products.

Iron ore is upgraded to higher iron content through concentration. The concentrate must be pelletized in order to feed a blast furnace or a DRI (direct reduction of iron ore) plant. Pellets are indurate spheres of ore with high iron content and uniform quality. Huge amount of broken pellets are wasted annually during the importing process from Brazil to Egypt, thus reducing the environmental impact of broken pellets will give their products further important benefits and offer significant potential for cost saving if they are reintroduced into the industrial process through well planned programs. Using broken pellets waste (BPW)

* Corresponding author.
E-mail: salwa_NRC@hotmail.com

in developing magnetic properties will be promising in the future. Several materials that have magnetic properties have been developed [1–6], and among them ferric and ferromagnetic glass ceramics have been investigated [7–10].

Glass ceramics are defined as composite materials that contain at least one crystalline phase dispersed in an amorphous glassy matrix. The chemical composition of the glass precursor influences the physical and chemical properties of the composite. Therefore, the investigation of new composite glass materials with controlled particle size distribution and aspect ratio is quite desirable. Preparation of magnetite-containing glass ceramics has been reported by several works [11–13]. Ferromagnetic bioglass ceramics containing 45 wt% of magnetite were prepared [14], and the ceramics with about 60 wt% of magnetite were reported by others [15,16]. Traditional compact magnetic materials are usually prepared by sintering of ferrite powders [17,18] with a mean particle size of about 1 μm at 1200–1250 ℃. During sintering, the magnetic crystals grow so that multi-domain behavior occurs and lowers the coercivity of the material [1]. On the other hand, glass ceramics are considered as a compact body in which magnetic particles are well dispersed and maintain the single domain behavior. Therefore, preparation of compact glass ceramics that contain single domain particles (< 100 nm) and are separated by a nonmagnetic matrix can lower the sinter temperature, prevent the particles from growing to multi-domain ones and cause low magnetic interaction.

Furthermore, spinel and hexaferrites (as the examples for soft and hard magnets in the same order, respectively) with the general formula MFe_2O_4 for spinel ferrites and $MFe_{12}O_9$ for hexaferrites (where M is a divalent cation) are large important classes of magnetic materials. The interesting magnetic properties of the spinel ferrites originate mainly from the magnetic interactions between cations with magnetic moments, which are situated in tetrahedral and octahedral sites [19–21]. These magnetic materials have wide applications in material science [22–27] and biotechnology [15,16,28]. Soft and hard nanomagnetic glass ceramics have great potential applications, especially in health care such as cell separation, magnetic resonance imaging contrast agents, drug delivery and hyperthermia treatment of cancer. In addition, they have a wide range of applications in information storage systems, ferrofluid technology [29], magneto caloric refrigeration, gas-sensors and as catalysts in some chemical engineering industries.

The main objective of this work is to study the possibility of utilization of iron oxide broken pellets waste from various metallurgical plants to prepare both soft and hard ferromagnetic glass ceramics which have great applications in different industries.

2 Experimental methods

2.1 Preparation of the glass

X-ray fluorescence (XRF) analysis of the BPW samples is illustrated in Table 1. In this work, the samples are prepared with two compositions: one based on crystallization of $ZnFe_2O_4$ as soft magnet, the other based on $BaFe_{12}O_{19}$ as hard magnet. The compositions of the prepared samples are illustrated in Table 2, where RS and RH are soft and hard magnetic reference samples respectively that are prepared from pure chemicals such as $ZnCO_3$, Na_2CO_3, $NH_4H_2PO_4$, TiO_2, $BaCO_3$, H_3BO_3 and SiO_2. Also, SMGC and HMGC are referred to soft magnetic glass ceramics that contain about 54% of BPW and hard magnetic glass ceramics that contain ~37% of BPW, respectively. Small amounts of ZnO as $ZnCO_3$, Na_2O as Na_2CO_3, P_2O_5 as $NH_4H_2PO_4$, TiO_2, BaO as $BaCO_3$ and B_2O_3 as H_3BO_3 are added to complete the design of the desired phases.

The samples were prepared by melting the required amounts of chemicals of reagent grade with composition shown in Table 2 in platinum crucibles at about 1500 ℃ for soft ferrite samples and around 1200 ℃ for hard ferrite ones. This process lasted for 2 h in electrically heated furnace with occasional swirling every 30 min to ensure homogenization. The melts were poured onto a stainless steel plate at room temperature and pressed into 1–2 mm thick strips by another cold steel plate.

2.2 Characterization

Differential thermal analysis (DTA), using SDTQ600 instrumentation under inert gas, was utilized to determine the temperatures of glass transition (T_g) and crystallization (T_c) of the glass samples. The heating rate was 10 ℃/min and alumina was used as inert reference material. The results obtained were used as a guide for determining the required heat-treatment temperatures needed to induce crystallization in the

Table 1 Quantitative XRF analysis of BPW

Main constituent	Weight percentage (wt%)
SiO_2	2.310
TiO_2	0.080
Al_2O_3	0.970
$Fe_2O_3^{tot}$	95.060
MgO	0.080
CaO	0.980
Na_2O	0.060
K_2O	0.020
P_2O_5	0.110
CuO	0.043
Cr_2O_3	0.069
MnO	0.002
SO_3	0.050
LOI	0.120
Cl	0.042

Table 2 Chemical composition of the prepared magnetic glass ceramics

Chemical composition	Sample			
	RS (wt%)	SMGC (wt%)	RH (wt%)	HMGC (wt%)
Fe_2O_3	70.50	65.5	43.17	34.97
SiO_2	—	1.6	4.64	4.50
TiO_2	2.21	0.005	—	0.03
ZnO	23.96	—	—	—
Al_2O_3	—	0.67	—	0.36
MgO	—	0.055	—	0.03
CaO	—	0.675	—	0.36
Na_2O	2.21	0.04	—	0.022
K_2O	—	0.014	—	0.00736
P_2O_5	1.10	4.21	—	0.04
CuO	—	0.03	—	0.016
Cr_2O_3	—	0.05	—	0.025
MnO	—	0.138	—	0.00074
B_2O_3	—	22.66	10.76	25.72
BaO	—	—	41.43	33.92

samples. Samples were heat treated at 900 ℃ for 2 h to investigate the effect of heat treatment on the phase transformation and in turn the sample properties.

Samples before and after heat treatment were subjected to powder X-ray diffraction using Ni-filled Cu Kα radiation for determination of their content and type of precipitated crystalline phases. X-ray diffraction (XRD) was performed using Bruker D8, an advanced instrument. The reference data for the interpretation of the XRD patterns was obtained from ASTM X-ray diffraction card files.

Samples were crushed and sonically suspended in ethanol. Few drops of the suspended solution were placed on an amorphous carbon film held by a copper micro grid mesh and then observed using JEM 2010 transmission electron microscope to study the microstructure and crystallite size.

The magnetic properties were studied using a vibrating sample magnetometer (VSM, 9600-1 LDJ, USA) in a maximum applied field of 20 kOe. From the obtained hysteresis loops, the saturation magnetization (M_s), remanance magnetization (M_r) and coercivity (H_c) were determined.

3 Results and discussion

3.1 Diffrential thermal analysis

DTA of RH, HMGC, RS and SMGC samples before heat treatment are illustrated in Fig. 1. Our materials are almost in a crystalline state as will be illustrated later using XRD analysis. When the amorphous state decreases, the endothermic and exothermic intensities will decrease too. In general, DTA results show lower intensity thermal effects due to the high degree of crystallization during cooling from the melting temperature to room temperature. DTA results show broad endothermic effects at 550 ℃ for RH, 536 ℃ for HMGC, 657 ℃ for RS and about 596 ℃ for SMGC. This endothermic reaction is believed to be caused by an increase in heat capacity due to transformation of glass from rigid to plastic structure and the accompanied rearranging of different atoms as a precrystallization step [30]. It is noticed that the endothermic temperatures are lowered in the batch compositions containing BPW than those of pure chemicals. Previous results can be attributed to the refluxing effect of different oxides present in BPW, as shown in Table 2, which lower the samples' viscosity and T_g as well. This endothermic effect is followed by two exothermic peaks at 611 ℃ and 737 ℃ for RH sample and at 591 ℃ and 698 ℃ for HMGC sample, which correspond to crystallization of Ba–hexaferrite. On the other hand, a single broad exotherm is appeared at 821 ℃ for SMGC sample to represent Zn–ferrite crystallization, as will be confirmed by X-ray later. The absence of exothermic effect in RS sample indicates high degree of crystallization during cooling from the melting temperature to room temperature. The shape and intensity of the exothermic peak are good mirror of the crystallization process; the sharper and stronger exothermic peak reflects larger and quicker crystallization, but if the exothermic peak is broad, the crystallization is slow and small [30].

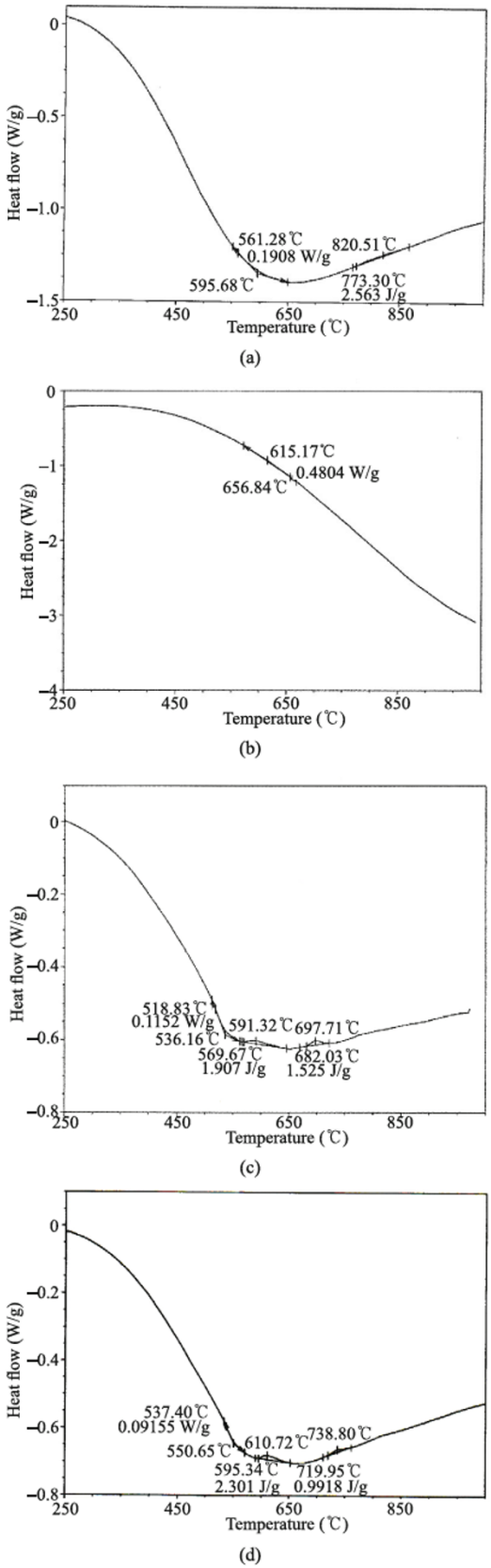

Fig. 1 DTA of (a) SMGC, (b) RS, (c) HMGC and (d) RH samples after quenching from the melting temperature.

According to the DTA results, heat treatment schedule was applied to samples at 900 ℃ for 2 h to study the effect of heat treatment on the crystallization process.

3.2 X-ray diffraction analysis

Figures 2 and 3 show the XRD results of samples under investigation before and after applying heat treatment schedule. In general, the major detectable peaks can be indexed to Zn–ferrite ($ZnFe_2O_4$) and Ba–hexaferrite ($BaFe_{12}O_{19}$) for SMGC and HMGC samples, respectively. This means the success of the designed compositions to reach the desired phases.

Figure 2 represents the XRD patterns of waste materials (BPW) and samples RS and SMGC before and after heat treatment. From Fig. 2(a), it is noticed that hematite (Fe_2O_3) is the only crystallizing phase in BPW, which is then converted to Zn–ferrite ($ZnFe_2O_4$) as a major phase with some traces of unconverted hematite in the designed SMGC before heat treatment. Larger amount of hematite relative to Zn–ferrite phase is crystallized in this sample after heat treatment at 900 ℃ for 2 h. The lower intensities of Zn–ferrite peaks (i.e., lower degree of crystallization) after heat treatment can be attributed to partial oxidation of Fe^{2+} into Fe^{3+} ions; consequently, a crystallization of large

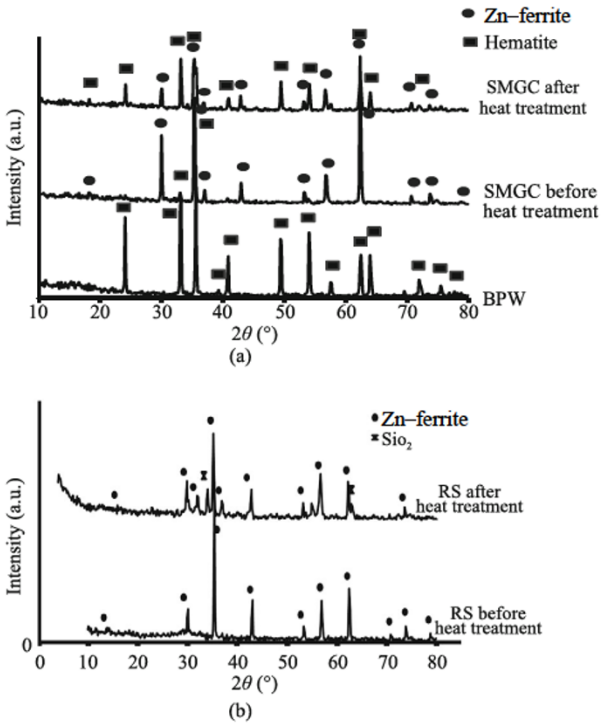

Fig. 2 XRD spectra for (a) BPW and SMGC and (b) RS samples before and after heat treatment.

amount of hematite at the expense of Zn–ferrite is noticed. The XRD spectra represent the crystallization of Zn–ferrite as a single phase in RS sample (Fig. 2(b)), but with a lower degree of crystallization relative to SMGC sample. The amount of Zn–ferrite is decreased in RS sample by applying heat treatment at 900 ℃ for 2 h due to the separation of SiO_2 phase.

Through comparing the composition of RS and SMGC, it is clear that there are extra oxides present in SMGC sample due to using BPW in the batch composition as listed in Table 2. These oxides facilitate the crystallization of Zn–ferrite through decreasing the viscosity of the sample leading to more mobility of ions to crystallize in quenched sample. The effect of heat treatment on SMGC is clear as Fe^{2+} are ions oxidized to Fe^{3+} leading to separation of more hematite crystals and reduction of Zn–ferrite crystallization affinity as reflected by its lower XRD intensities.

On the other hand, Fig. 3(a) shows the XRD spectra of HMGC before and after heat treatment. It can be noticed that the pure hematite phase present in BPW sample disappears and a broad hump characterizing the amorphous glassy nature appears in HMGC sample before heat treatment, while Ba–hexaferrite crystallizes as the sole formed magnetic phase in a nonmagnetic matrix when the sample is subjected to heat treatment at 900 ℃ for 2 h. A clear effect of the heat treatment at 900 ℃ for 2 h on RH sample (Fig. 3(b)), marks the transformation from amorphous to crystalline state and is mirrored by crystallization of pure Ba–hexaferrite. Obviously, HMGC crystallizes much more amount of Ba–hexaferrite than that crystallized in RH which is reflected by higher XRD peak intensities.

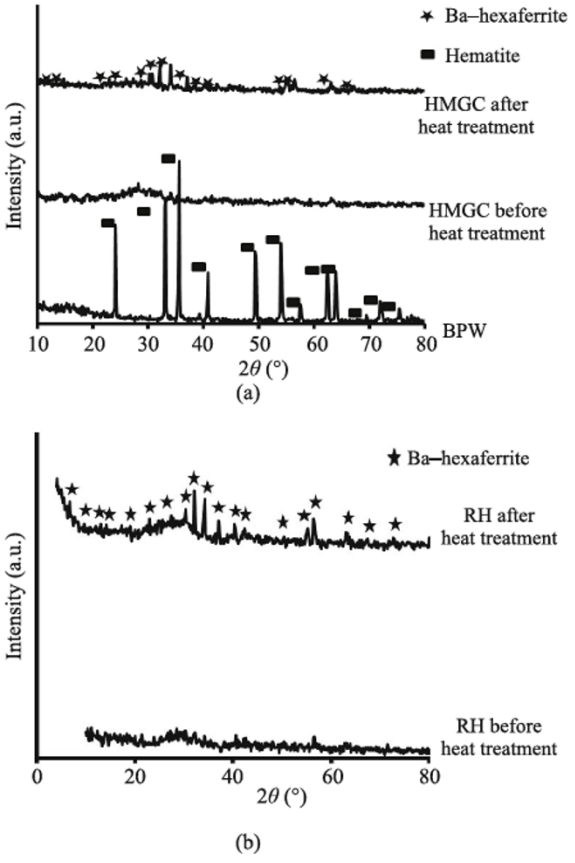

Fig. 3 XRD spectra for (a) BPW and HMGC and (b) RH samples before and after heat treatment.

3.3 Transmission electron microscopy

Transmission electron microscopy (TEM) was performed in order to investigate the possibility of micro twinning and the homogeneity of the materials. Particle size measurements can be viewed from TEM measurements, in a sense of approximation. Figure 4 shows the TEM microstructures in high magnification for SMGC, HMGC, RH and RS samples before and after heat treatment. Figure 4(a) reveals the precipitation of nanosized cubic crystals of Zn–ferrite as a major phase in SMGC sample before heat treatment with crystallite size range of 15–20 nm. About 50% of the Zn–ferrite phase is transformed to hematite after heat treatment (Fig. 4(b)), causing the presence of different crystallite sizes (4 nm and 11 nm); this result agrees well with the XRD results (Fig. 2). On the other hand, it has been investigated from TEM results that Ba–hexaferrite with hexagonal crystals is formed as a unique phase with crystallite size range of 5–12 nm in HMGC sample after heat treatment (Fig. 4(d)) as given by the XRD results (Fig. 3). TEM for RS sample (Fig. 4(f)) shows the particle size around 223 nm after heat treatment. In addition, TEM of RH sample (Fig. 4(h)) shows the crystallization of Ba–hexaferrite as a single phase with crystalline size in the range of 2–12 nm after heat treatment.

3.4 Magnetic properties

Figures 5 and 6 depict the room temperature magnetic hysteresis (M–H) loops of RS, SMGC, RH and HMGC samples before and after heat treatment under a magnetic field strength of 20 kOe. Table 3 displays the relevant magnetic parameters: saturation magnetization (M_s), coercivity (H_c) and remanence (M_r) obtained from M–H loops. In general, the magnetic field necessary to saturate the samples increases with the increase in the crystallization of Zn–ferrite in soft samples and

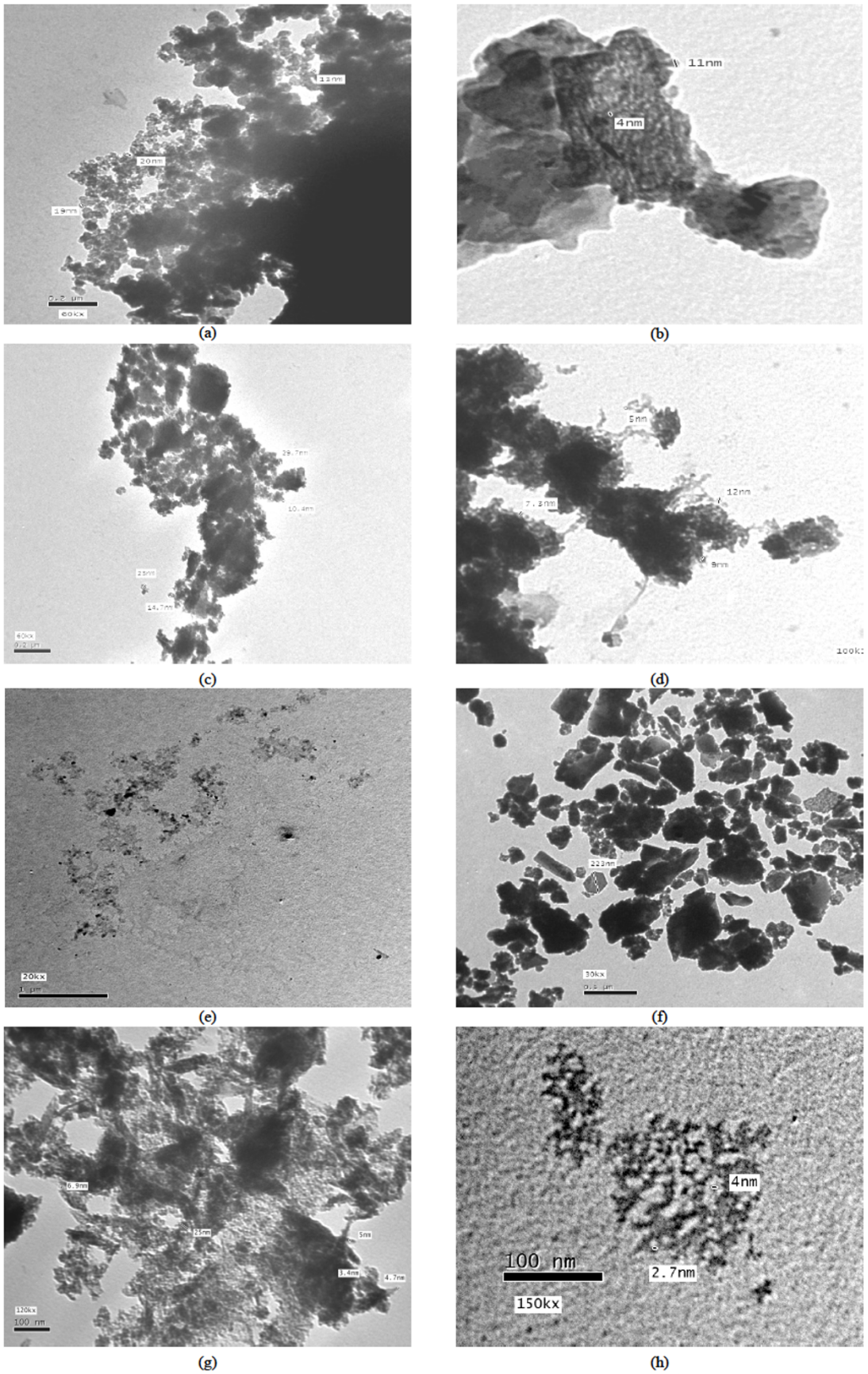

Fig. 4 TEM of (a) quenched SMGC, (b) heat treated SMGC, (c) quenched HMGC, (d) heat treated HMGC, (e) quenched RS, (f) heat treated RS, (g) quenched RH and (h) heat treated RH samples.

Ba–hexaferrite in hard magnets. Figure 5 demonstrates that, M_s is increased from 1.0406 emu/g for the original raw material sample BPW, to 77.185 emu/g for SMGC sample before heat treatment and reduced to 8.9269 emu/g for SMGC sample after heat treatment. On the other hand, Fig. 5 demonstrates that the magnetization of RS sample declines from 38.678 emu/g to 24.293 emu/g after being subjected to heat treatment at 900 ℃ for 2 h. In addition, Fig. 6 shows that M_s is increased from 1.0406 emu/g for the original raw material sample BPW to 7.6175 emu/g for HMGC sample before heat treatment and increased to 21.575 emu/g for this sample subjected to heat treatment. The same trend is noticed from Fig. 6 where M_s of RH sample increases from 8.0774 emu/g to 16.665 emu/g after heat treatment at 900 ℃ for 2 h. As expected, saturation magnetization in the samples is directly proportional to the degree and amount of crystallization of Zn–ferrite and Ba–hexaferrite. It should be considered that Zn–ferrite and Ba–hexaferrite are ferromagnetic materials, whereas hematite is an antiferrimagnetic. From the experimental data, it is seen that hematite and amorphous phases have a very low saturation magnetization. As a consequence, the variation of the saturation magnetization can be attributed to the modification of the quantity of Zn–ferrite and Ba–hexaferrite crystals [31] present in the glass ceramic samples. Therefore, the maximum magnetization values are 77.185 emu/g for SMGC before heat treatment and 21.575 emu/g for HMGC after heat treatment, indicating the heaviest and most intense Zn–ferrite and Ba–hexaferrite crystallization of all the soft and hard magnet samples respectively. Bretcanu *et al*. [32] found that, 1 g of ferromagnetic glass ceramics which have saturation magnetization 30 emu/g and coercive force 220 Oe can increase the temperature of 20 ml distilled water after 2 min of applying magnetic field to about 40 ℃. Thus in this work, the studied ferromagnetic glass ceramic sample with saturation magnetization 77.185 emu/g for SMGC before heat treatment is expected to increase this temperature to higher than 40 ℃, and this will be more effective for biomedical applications. Magnetic anisotropy, shape and dimension of the crystals, residual stress and crystal imperfection influence the coercivity and remanence magnetization [33].

The coercivity of soft ferrimagnetic glass ceramics has a wide range varied between 357.49 Oe for the

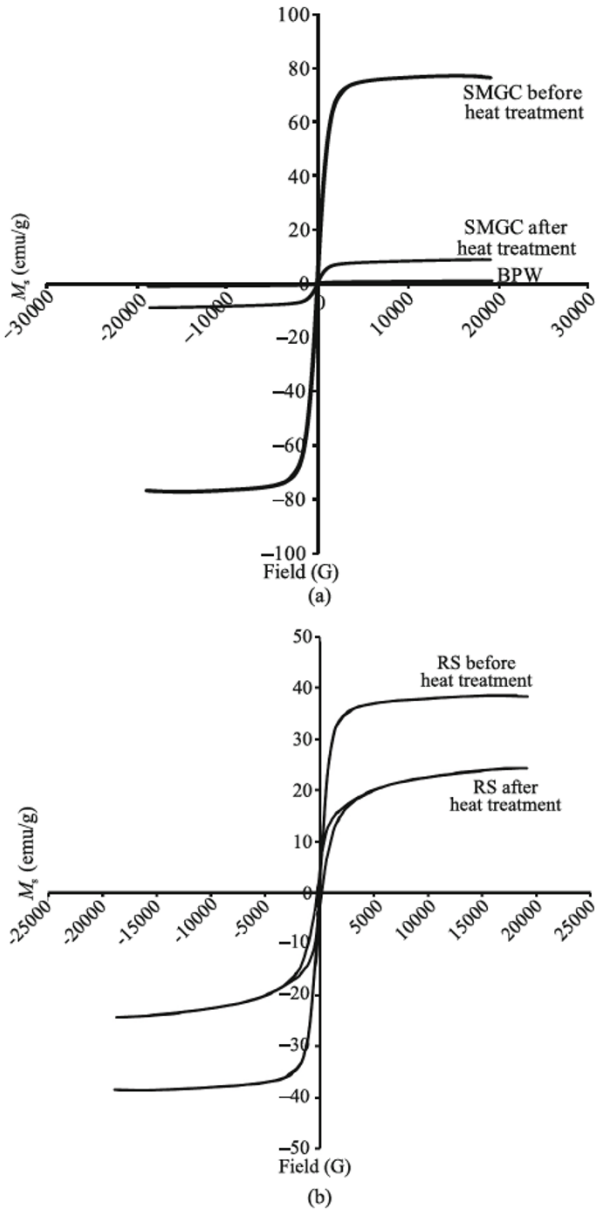

Fig. 5 Magnetization curves for BPW, SMGC and RS samples before and after heat treatment.

original sample BPW and 14.856 Oe for SMGC before heat treatment with a little increase to 24.499 Oe after heat treatment. The same variation takes place in HMGC sample as it declines from 357.49 Oe for the original sample to 266.34 Oe for HMGC sample before heat treatment and increases to 449.10 Oe after heat treatment. In addition, heat treatment has a noticeable high effect on the reference samples' coercivity as it increases from 16.756 Oe for RS to 193.44 Oe after heat treatment and jumpes from 160.39 Oe for RH to 1001.5 Oe after heat treatment. The coericivity of a ferrimagnetic material is the intensity of the applied

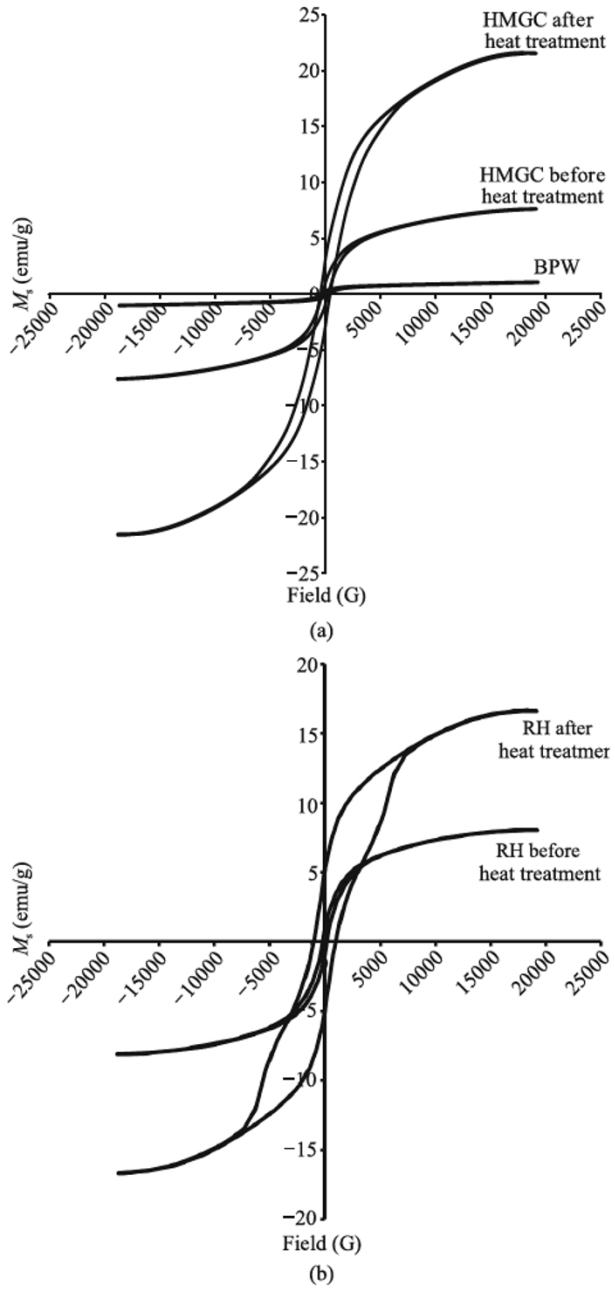

Fig. 6 Magnetization curves for BPW, HMGC and RH samples before and after heat treatment.

magnetic field required to reduce the magnetization of that material to zero after the magnetization of the sample has been driven to saturation. Coericivity measures the resistance of a ferromagnetic material to become demagnetized. The wide range of coericivity gives a wide range of applications. Materials with high coericivity which are called hard ferromagnetic materials are used to make permanent magnets. Permenant magnets find applications in electric motors, magnetic recording media (e.g., hard drives, floppy disks or magnetic tapes) and magnetic separation. While materials with low coericivity which are said to be soft magnets may be used in microwave devices, magnetic shielding, transformers or recording heads.

The retentivity is found to detect the amount of magnetic materials which can be magnetized [34], even in the absence of external magnetic field. In comparison between soft and hard ferrites, Table 3 shows clearly that the retentivity of all the hard magnets is larger than that of the soft ones which means that the area of the hysteresis loops of hard ferrites is larger than the area in the case of soft ferrites. The area under the hysteresis loop is proportional to the energy loss and hence the heat generated by a sample under an alternating field; hard ferrite samples are capable of generating more heat. The large variation in the area under the loops for hard and soft ferrite samples provides a means for controlled heat generation by appropriate choice of sample.

4 Conclusions

Two different ferrimagnetic glass ceramics with compositions based on crystallization of Zn–ferrite as soft magnet and Ba–hexaferrite as hard magnet were prepared. The influences of chemical composition, the amount of crystallized Zn–ferrite and Ba–hexaferrite and the microstructure of ferromagnetic glass ceramics on magnetic properties of glass ceramics were investigated. Heat treatment schedule at 900 ℃ for 2 h had a negative effect on Zn–ferrite crystallization in soft glass ceramics. On the contrary, subjecting hard ferrites to heat treatment increased the amount of Ba–hexaferrite crystallization, which was proved by TEM analysis. From the magnetic measurements, we conclude that the maximum values were 77.185 emu/g

Table 3 Magnetic properties of BPW, RS, RH, SMGC and HMGC glass ceramics before and after heat treatment

Sample	Magnetization (emu/g)	Coercivity (Oe)	Retentivity (emu/g)
BPW	1.0406	357.49	0.22056
RS	38.678	16.756	0.73946
SMGC	77.185	14.856	0.99761
RS 900 ℃ for 2 h	24.293	193.44	3.70140
SMGC 900 ℃ for 2 h	8.9269	24.499	0.19882
RH	8.0774	160.39	0.92542
HMGC	7.6175	266.34	0.95882
RH 900 ℃ for 2 h	16.665	1001.5	5.03920
HMGC 900 ℃ for 2 h	21.575	449.10	2.96680

for SMGC before heat treatment and 21.575 emu/g for HMGC after heat treatment, and these reflected the heaviest and most intense Zn–ferrite and Ba–hexaferrite crystallization of all the soft and hard magnet samples respectively. Samples' coericivity increased by subjecting them to heat treatment. In addition, the retentivity of all hard magnets showed larger value than that of the soft ones.

References

[1] Cetas TC, Gross EJ, Contractor Y. A ferrite core/metallic sheath thermoseed for interstitial thermal therapies. *IEEE T Bio-med Eng* 1998, **45**: 68–77.

[2] Jordan A, Scholz R, Wust P, *et al*. Magnetic fluid hyperthermia (MFH): Cancer treatment with AC magnetic field induced excitation of biocompatible superparamagnetic nanoparticles. *J Magn Magn Mater* 1999, **201**: 413–419.

[3] Gómez-Lopera SA, Plaza RC, Delgado AV. Synthesis and characterization of spherical magnetite/ biodegradable polymer composite particles. *J Colloid Interface Sci* 2001, **240**: 40–47.

[4] Lee YK, Kim DH, Lee YJ, *et al*. Ceramics, cells and tissues. Eighth Annual Seminar and Meeting, Faenza, 2003.

[5] Takegami K, Sano T, Wakabayashi H, *et al*. New ferromagnetic bone cement for local hyperthermia. *J Biomed Mater Res A* 1998, **43**: 210–214.

[6] Borrelli NF, Young PL. Positive imaging method using doped silver halide medium. US Patent 4,323,640. 1982.

[7] Kokubo T, Yamamuro T, Ebisawa Y, *et al*. European Patent 361797. 1990.

[8] Oh S-H, Choi S-Y, Lee Y-K, *et al*. Research on annihilation of cancer cells by glass–ceramics for cancer treatment with external magnetic field. I. Preparation and cytotoxicity. *J Biomed Mater Res A* 2001, **54**: 360–365.

[9] Ebisawa Y, Miyaji F, Kokubo T, *et al*. Surface reaction of bioactive and ferrimagnetic glass–ceramics in the system $FeO–Fe_2O_3–CaO–SiO_2$. *J Ceram Soc Jpn* 1997, **105**: 947–951.

[10] Arcos D, del Real RP, Vallet-Regí M. A novel bioactive and magnetic biphasic material. *Biomaterials* 2002, **23**: 2151–2158.

[11] Ebisawa Y, Miyaji F, Kokubo T, *et al*. Bioactivity of ferrimagnetic glass–ceramics in the system $FeO–Fe_2O_3–CaO–SiO_2$. *Biomaterials* 1997, **18**: 1277–1284.

[12] O'Horo M, Steinitz R. Characterization of devitrification of an iron-containing glass by electrical and magnetic properties. *Mater Res Bull* 1968, **3**: 117–125.

[13] Auric P, Van Dang N, Bandyopadhyay AK, *et al*. Superparamagnetism and ferrimagnetism of the small particles of magnetite in a silicate matrix. *J Non-Cryst Solids* 1982, **50**: 97–106.

[14] Bretcanu O, Spriano S, Verné E, *et al*. The influence of crystallised Fe_3O_4 on the magnetic properties of coprecipitation-derived ferrimagnetic glass–ceramics. *Acta Biomater* 2005, **1**: 421–429.

[15] Abdel-Hameed SAM, Hessien MM, Azooz MA. Preparation and characterization of some ferromagnetic glass–ceramics contains high quantity of magnetite. *Ceram Int* 2009, **35**: 1539–1544.

[16] Abdel-Hameed SAM, El Kady AM. Effect of different additions on the crystallization behavior and magnetic properties of magnetic glass–ceramic in the system $Fe_2O_3–ZnO–CaO–SiO_2$. *J Adv Mater* 2012, **3**: 167–175

[17] Shirk BT, Buessem WR. Magnetic properties of barium ferrite formed by crystallization of a glass. *J Am Ceram Soc* 1970, **53**: 192–196.

[18] Gornert P, Sinn E, Schuppel W, *et al*. Structural and magnetic properties of $BaFe_{12-2x}Co_xTi_xO_{19}$ powders prepared by the glass crystallization method. *IEEE T Magn* 1990, **26**: 12–14.

[19] Evans BJ, Hafner SS, Weber HP. Electric field gradients at ^{57}Fe in $ZnFe_2O_4$ and $CdFe_2O_4$. *J Chem Phys* 1971, **55**: 5282.

[20] Ata-Allah SS, Fayek MK. Effect of Cu substitution on conductivity of Ni–Al ferrite. *J Phys Chem Solids* 2000, **61**: 1529–1534.

[21] Mahmoud MH, Hamdeh HH, Ho JC, *et al*. Mössbauer studies of manganese ferrite fine particles processed by ball-milling. *J Magn Magn Mater* 2000, **220**: 139–146.

[22] Müller R, Ulbrich C, Schüppel W, *et al*. Preparation and properties of barium-ferrite-containing glass ceramics. *J Eur Ceram Soc* 1999, **19**: 1547–1550.

[23] Lee C-K, Speyer RF. Glass formation and crystallization of barium ferrite in the $Na_2O–BaO–Fe_2O_3–SiO_2$ system. *J Mater Sci* 1994, **29**: 1348–1351.

[24] Sohn S-B, Choi S-Y, Shim IB. Preparation of

Ba–ferrite containing glass–ceramics in BaO–Fe_2O_3–SiO_2. *J Magn Magn Mater* 2002, **239**: 533–536.

[25] Rezlescu L, Rezlescu E, Popa PD, *et al*. Fine barium hexaferrite powder prepared by the crystallisation of glass. *J Magn Magn Mater* 1999, **193**: 288–290.

[26] Görnert P, Sinn E, Rösler M. Crystalline materials: Growth and characterization. *Key Eng Mat* 1991, **58**: 129–148.

[27] Abdel-Hameed SAM, Marzouk MA, Abdel-Ghany AE. Magnetic properties of nanoparticles glass–ceramic rich with copper ions. *J Non-Cryst Solids* 2011, **357**: 3888–3896.

[28] Safarikova M, Safarik I. The application of magnetic techniques in biosciences. *Magnetic and Electrical Separation* 2001, **10**: 223–252.

[29] Sharifi I, Shokrollahi H, Amiri S. Ferrite-based magnetic nanofluids used in hyperthermia applications. *J Magn Magn Mater* 2012, **324**: 903–915.

[30] El-Shennawi AWA, Moris MM, Khater GA, *et al*. Thermodynamic investigation of crystallization behaviour of pyroxenic basalt-based glasses. *J Therm Anal Calorim* 1998, **51**: 553–560.

[31] Roy MK, Haldar B, Verma HC. Characteristic length scales of nanosize zinc ferrite. *Nanotechnology* 2006, **17**: 232.

[32] Bretcanu O, Verné E, Cöisson M, *et al*. Temperature effect on the magnetic properties of the coprecipitation derived ferrimagnetic glass–ceramics. *J Magn Magn Mater* 2006, **300**: 412–417.

[33] Cullity RD. *Introduction of Magnetic Materials*. Addison-Wesley, 1972.

[34] Abdel-Hameed SAM, Elwan RL. Effect of La_2O_3, CoO, Cr_2O_3 and MoO_3 nucleating agents on crystallization behavior and magnetic properties of ferromagnetic glass–ceramic in the system Fe_2O_3·CaO·ZnO·SiO_2. *Mater Res Bull* 2012, **47**: 1233–1238.